

Electronic spectroscopy of the $\tilde{A}^1A'' \leftarrow \tilde{X}^1A'$ system of CDF†

Chong Tao, Mihaela Deselnicu, Haiyan Fan, Calvin Mukarakate, Ionela Ionescu and Scott A. Reid*

Received 19th October 2005, Accepted 22nd December 2005

First published as an Advance Article on the web 10th January 2006

DOI: 10.1039/b514826j

To further investigate the Renner–Teller (RT) effect and barriers to linearity and dissociation in the simplest singlet carbene, we recorded fluorescence excitation spectra of bands involving the pure bending levels 2_0^n with $n = 0-9$ and the combination states $1_0^1 2_0^n$ with $n = 1-8$ and $2_0^1 3_0^1$ with $n = 0-5$ in the $\tilde{A}^1A'' \leftarrow \tilde{X}^1A'$ system of CDF, in addition to some weak hot bands. The spectra were measured under jet-cooled conditions using a pulsed discharge source, and rotationally analyzed to yield precise values for the band origins and rotational constants; fluorescence lifetimes were also measured to probe for lifetime lengthening effects due to the RT interaction. The derived \tilde{A} state parameters are compared with previous results for CHF and with predictions of *ab initio* electronic structure theory. The approach to linearity in the \tilde{A} state is evidenced in a sharp increase in the A rotational constant with bending excitation, and a minimum in the vibrational intervals near 2^9 . A fit of the vibrational intervals for the pure bending levels yields an \tilde{A} state barrier to linearity in good agreement both with that previously derived for CHF and *ab initio* predictions. From the spectra and lifetime measurements, the onset of extensive RT perturbations is found to occur at a higher energy than in CHF, consistent with the smaller A constant.

Introduction

Simple carbenes are important in many areas of chemistry,¹⁻⁶ and there is intense current interest in the spectroscopy, photochemistry, and photophysics of these species. As the smallest carbenes with singlet ground states, the monohalocarbenes CHX (X = F, Cl, Br) have received significant attention.⁷⁻⁷¹ These are prototypical systems in several respects: first, for understanding the spectroscopy, dynamics, and electronic structure of singlet carbenes; second, for benchmark comparisons of experimental and *ab initio* singlet–triplet gaps; and third, for study of the Renner–Teller (RT) effect, as the two lowest lying singlet states are components of a RT pair which correlate with a $^1\Delta$ state in the linear configuration.^{7,8} Focusing on the latter, we and others have recently shown that CHF is a prototypical system due to the high barrier to linearity ($\sim 6300 \text{ cm}^{-1}$) in the excited state, which affords the opportunity to systematically view the onset of RT interactions as the barrier is approached.^{44,47,64,66-70} In contrast, the excited state barriers are much smaller for CHCl and CHBr,^{7,39,40,52,56} and RT interactions are observed even in the origin bands of these systems.^{39,40,52} We note that the dihalocarbene CCl_2 is also an excellent system for systematic study of RT interactions,⁷² although complicated by the presence of strong anharmonic resonances in the excited state.

In recent articles, we reported studies of the $\tilde{A}^1A'' \leftarrow \tilde{X}^1A'$ system of CHF using a combination of fluorescence excitation

spectroscopy, polarization quantum beat spectroscopy (QBS), fluorescence lifetime measurements, and dispersed fluorescence (DF) spectroscopy.^{64,66-70} First, we showed that the lifetimes of upper state levels with $K_a \geq 1$ display an obvious lengthening with increasing energy, due to the RT interaction, which provides a textbook example of lifetime lengthening.⁶⁴ We recorded fluorescence excitation spectra of the bands 2_0^n ($n = 0-7$), $1_0^1 2_0^n$ ($n = 1-6$), and $2_0^1 3_0^1$ ($n = 0-3$); the derived term energies and \tilde{A} state parameters were in excellent agreement with the predictions of *ab initio* electronic structure theory.⁶⁶ The approach to linearity in the \tilde{A} state was evidenced in a sharp increase in the A rotational constant with bending excitation, as first reported by Kable and co-workers,⁴⁷ and a minimum in the vibrational intervals near 2^7 . We derived a barrier height of $6300 \pm 270 \text{ cm}^{-1}$, consistent with a theoretical prediction of 6770 cm^{-1} ,⁴⁴ and placed a lower limit on the \tilde{A} state barrier to dissociation of $\sim 8555 \text{ cm}^{-1}$ above the vibrationless level, consistent with a theoretical prediction of $\sim 8955 \text{ cm}^{-1}$.⁴⁴

Our subsequent studies used polarization and Zeeman QBS to probe the ^{19}F and ^1H nuclear hyperfine structure and perturbations in the $\tilde{A}^1A'' \leftarrow \tilde{X}^1A'$ system.⁶⁷⁻⁶⁹ We determined the nuclear spin-rotation constants (C_{aa}) and weak field Lande g_{aa} factors of many \tilde{A}^1A'' state levels. Consistent with a two-state model, the majority of observed levels exhibit a linear correlation of C_{aa} and g_{aa} , and our analysis yielded effective (\bar{a}) hyperfine constants for the ^{19}F and ^1H nuclei of 728(23) and 55(2) MHz, respectively.⁶⁸ The latter was determined for the first time, owing to the high resolving power of QBS. We then focused on the $K_a = 1 \leftarrow 0$ sub-band of 2_0^4 , which is perturbed by both RT and spin–orbit interactions.⁶⁹ We showed that RT induced mixing with a high vibrational

Department of Chemistry, Marquette University, Milwaukee, WI 53201-1881, USA. E-mail: scott.reid@mu.edu

† Electronic supplementary information (ESI) available: Observed and calculated line positions for bands in the CDF $\tilde{A}^1A'' \leftarrow \tilde{X}^1A'$ system. See DOI: 10.1039/b514826j

level of \tilde{X}^1A' leads to a splitting of this sub-band. The higher energy member is free of rotational perturbations, and exhibits very *small* Lande g -factors and hyperfine constants, which we explained within a model that incorporates only the $\tilde{A}^1A'' \leftarrow \tilde{X}^1A'$ interaction.⁶⁹ In contrast, every line in the lower energy sub-band is perturbed by spin-orbit mixing with background levels of \tilde{a}^3A'' , as evidenced by large ^{19}F and ^1H hyperfine constants and Lande g -factors. Analysis of this sub-band, in concert with density functional theory (DFT) calculations, yielded the first information on the ^{19}F and ^1H hyperfine structure of the \tilde{a}^3A'' state and the magnitude of the spin-orbit matrix elements.

In comparison with CHF, little is known about the deuterated isotopomer CDF. The primary motivation for study of the electronic spectroscopy of CDF is to gain additional insight into the RT interaction and the excited state barrier to linearity. As discussed by Duxbury,⁷³ the RT effect for considerably bent component states can be viewed as an “electronic” Coriolis interaction with matrix elements of the form: $\langle \tilde{X}^1A' | AL_a | \tilde{A}^1A'' \rangle K$, where A is the a -axis rotational constant and L_a is the angular momentum operator (note that a -axis rotation correlates with vibrational angular momentum in the linear molecule). Thus, the CH(D)F system is an excellent one for probing the A dependence of the RT interaction. Indeed, while the 0_0^0 band of CHF displays a number of perturbations, particularly for higher K_a states,¹⁸ Hirota and co-workers reported a high resolution fluorescence excitation spectrum of the 0_0^0 band of CDF which was almost free of perturbations.¹⁹ In CHF, we found that RT interactions increase with energy as the barrier is approached;⁶⁶ of course, there are strong local perturbations such as those observed for 2^4 .^{66,69} In CDF, these will obviously change as different states are tuned in resonance; however, we wish to learn whether the onset of strong RT effects occurs at a similar energetic threshold. Another factor which may influence the magnitude of coupling matrix elements is the vibrational quantum number (n) at the RT intersection; n equals ~ 7 for CHF and ~ 9 for CDF.

In this study, then, we report our analysis of fluorescence excitation spectra and lifetimes of bands in the $\tilde{A}^1A'' \leftarrow \tilde{X}^1A'$ system of CDF. Our results are compared with previous results for CHF and with the predictions of *ab initio* electronic structure theory to gain further insight into the electronic structure of and RT effect in this prototypical singlet carbene.

Experimental

The apparatus, pulsed discharge nozzle, and data acquisition procedures have been described in detail in earlier studies.^{64–70} CDF was generated by a pulsed electrical discharge through a ~ 1 –2% mixture of CD_3F in argon that was premixed in a stainless steel cylinder. The typical backing pressure was ~ 1 –2 bar. The discharge was initiated by a +800–1200 V pulse of 10–50 μs duration, through a current limiting 10–100 k Ω ballast resistor. The timing of laser, nozzle, and discharge firing was controlled by a digital delay generator (Stanford Research Systems DG535), which also generated a variable width gate pulse for the high voltage pulser (Directed Energy GRX-1.5K-E). The laser system was an etalon narrowed dye

laser (Lambda-Physik Scanmate 2E) pumped by the second or third harmonic of a Nd:YAG laser (Continuum Powerlite 7010 or NY-61). For access to wavelengths below 430 nm, the fundamental dye output was mixed with the Nd:YAG fundamental in a BBO crystal. The laser beam was not focused, and typical pulse energies were ~ 1 mJ in a ~ 3 mm diameter beam. A portion of the dye laser fundamental was sent into a Fe–Ne or Fe–Ar lamp for absolute wavelength calibration using the optogalvanic effect. When the frequency mixing scheme was employed, the Nd:YAG fundamental frequency (9397.44 cm^{-1}) was determined by optogalvanic measurement of both the dye fundamental and sum frequency.

These measurements utilized a mutually orthogonal geometry of laser, molecular beam, and detector, where the laser beam crossed the molecular beam at a distance of ~ 10 mm (12.5 nozzle diameters) downstream. Fluorescence was collected and collimated by a $f/2.4$ plano-convex lens, and focused onto a photomultiplier tube detector (PMT) using a $f/3.0$ plano-convex lens. The fluorescence was filtered *via* an appropriate long-pass cutoff filter (Corion) prior to striking the PMT, which was held at typically -600 V. In acquiring fluorescence excitation spectra, the PMT signal was terminated into 15 k Ω and digitized by a fast oscilloscope (HP 54521A), and twenty laser shots were averaged at each step in wavelength (0.001 nm).

Transition frequencies were determined by fitting isolated lines to a Gaussian lineshape function, using a nonlinear least squares fitting routine in Origin 7.5 software. The transition frequencies were then fit to a standard asymmetric top Hamiltonian using a least squares routine in the AsyrotWin program package of Judge and Clouthier,⁷⁴ incorporating the ground state rotational constants determined in the high resolution study of Hirota and co-workers.¹⁹

CD_3F was synthesized from CD_3OD (Cambridge Isotope Labs, $>99\%$ D) *via* a literature procedure.⁷⁵

Results and discussion

Rotational analysis

We obtained and rotationally analyzed fluorescence excitation spectra of 21 cold bands in the progressions 2_0^0 ($n = 0$ –9), $1_0^1 2_0^0$ ($n = 1, 3$ –8), and $2_0^0 3_0^0$ ($n = 1$ –5), and several hot bands. The fit parameters for the cold bands are listed in Table 1, and Fig. 1 displays a comparison of experimental and simulated spectrum for the 0_0^0 band, which was free of perturbations over the range of J values accessed in our experiment. The upper state rotational constants determined for this band are identical to those of Hirota and co-workers¹⁹ within our uncertainties, although the number of transitions observed in our jet-cooled spectrum was far smaller.

With increasing energy, perturbations can be identified in sub-bands with $K'_a \geq 1$. This is illustrated in Fig. 2, which displays spectra for the 2_0^0 bands with $n = 0$ –8. Scattered rotational perturbations are observed for $n > 4$, and with increasing n the sub-bands with $K'_a \geq 1$ show strongly perturbed rotational structure with an associated decrease in intensity. For $n \geq 8$, only sub-bands terminating in $K'_a = 0$ can be observed. The perturbations can be grouped into two

Table 1 Fit parameters (in cm^{-1}) for the CDF(\tilde{A}^1A'') cold bands measured in this work

Band	T	A'	$(B' + C')/2$	$(B' - C')/2$	Δ'_K	N^b	σ^c
0_0^0	17 298.23(2) ^a	15.088(11)	0.9786(13)	0.0350(13)	0.0147(12)	75	0.027
2_0^1	18 085.18(13)	16.499(65)	0.9791(25)	0.0377(25)	0.063(15)	68	0.056
3_0^1	18 552.28(3)	15.098(8)	0.9690(17)	0.0353(17)	0.0147 ^d	83	0.040
2_0^2	18 864.06(15)	19.274(77)	0.9793(32)	0.0305(32)	0.226(17)	62	0.055
2_0^3	19 323.35(15)	16.407(64)	0.9709(37)	0.0323(37)	0.070(15)	52	0.045
2_0^4	19 633.82(8)	20.29(11)	0.9792(39)	0.0453(39)	0.112(25)	57	0.080
2_0^5	20 086.49(6)	18.182(93)	0.9816(16)	—	0.019(22)	51	0.069
1_0^2	20 178.00(8)	16.420(11)	0.9920(14)	—	0.102(24)	69	0.087
2_0^6	20 394.15(7)	24.43(10)	0.9828(44)	0.0303(44)	0.408(24)	54	0.075
2_0^7	20 827.84(5)	—	0.9817(12)	—	—	18	0.044
2_0^8	21 145.58(4)	30.007(46)	0.9798(34)	—	—	32	0.041
1_0^3	21 701.88(5)	20.777(50)	0.9755(22)	—	—	36	0.048
2_0^9	21 887.13(7)	37.569(19)	0.9866(30)	—	—	27	0.059
2_0^{10}	22 341.87(4)	—	0.9695(16)	—	—	18	0.036
1_0^4	22 447.90(4)	—	0.9761(13)	—	—	18	0.035
2_0^{11}	22 620.33(3)	—	0.9831(14)	—	—	17	0.025
1_0^5	23 183.35(3)	—	0.9765(69)	—	—	22	0.027
2_0^{12}	23 347.44(5)	—	0.9815(55)	0.0215(55)	—	20	0.036
1_0^6	23 909.92(2)	—	0.9750(74)	—	—	18	0.016
2_0^{13}	24 072.37(5)	—	0.9886(36)	—	—	12	0.036
1_0^7	24 629.07(3)	—	0.9980(12)	—	—	14	0.278
1_0^8	25 345.19(8)	—	0.9762(55)	—	—	11	0.055

^a Three standard errors given in parentheses. ^b Number of transitions included in the fit. ^c Standard deviation of the fit. ^d Fixed in the fit.

types: (1) RT interactions, which only affect states with $K'_a \geq 1$ and give rise to a lengthening in fluorescence lifetime relative to states with $K'_a = 0$, as illustrated in Fig. 3; and (2) spin-orbit interactions with background levels of the \tilde{a}^3A'' state. As

we have shown for CHF,⁶⁶ these can be differentiated using polarization QBS, and a detailed investigation of perturbations in this system using QBS will be the subject of a future report.

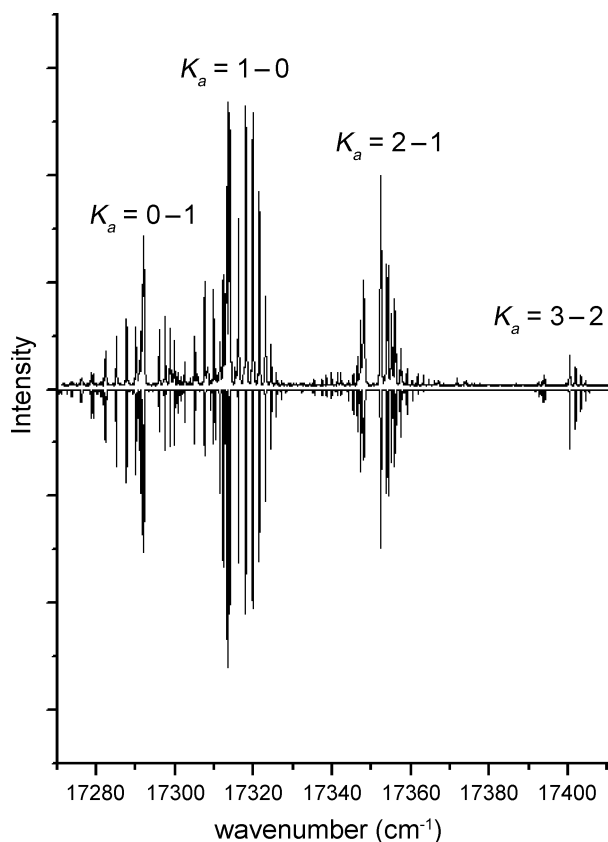


Fig. 1 Experimental (top) and simulated fluorescence excitation spectrum of the 0_0^0 band in the $\tilde{A}^1A'' \leftarrow \tilde{X}^1A'$ system of CDF.

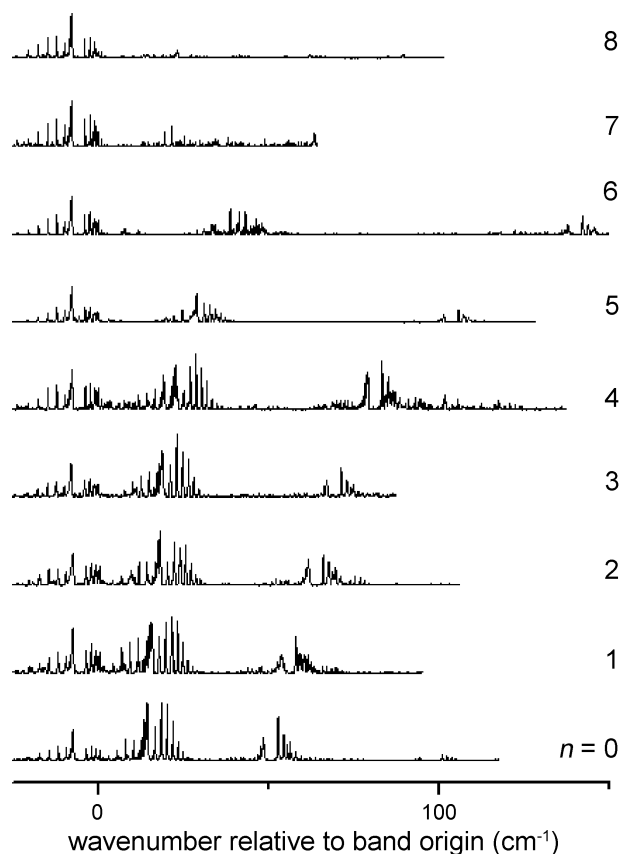


Fig. 2 Fluorescence excitation spectra of the pure bending levels $2_n''$ ($n = 0-8$) of CDF. See Fig. 1 for assignments of specific subbands.

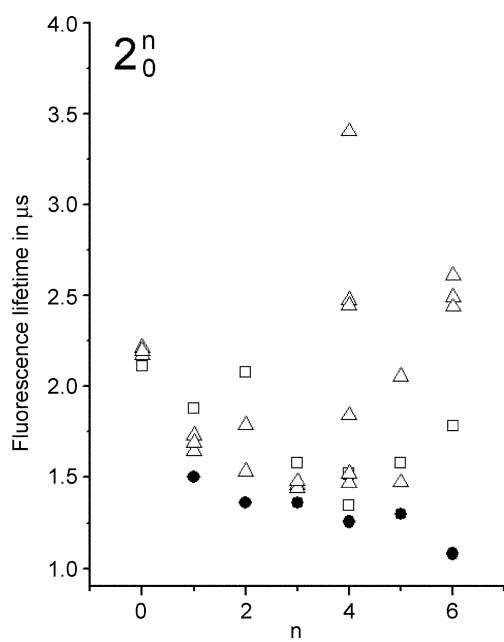


Fig. 3 Fluorescence lifetimes of the pure bending levels in CDF (\tilde{A}^1A''). The error bars are in each case smaller than the symbol size. Legend: ●, $K' = 0$; □, $K' = 1$; △, $K' = 2$.

It is instructive to compare Fig. 2 with analogous data for CHF. In the latter, the onset of extensive RT interactions, as evidenced in a strongly perturbed rotational structure for $K'_a \geq 1$, occurs near the 2^4 level, or $\sim 4000 \text{ cm}^{-1}$ above the vibrationless level. In CDF, the onset occurs near 2^6 , or $\sim 4600 \text{ cm}^{-1}$ above the zero point level. Qualitatively, this increase in threshold is consistent with the smaller A constant for CDF (CHF 2^4 , $A = 51.8 \text{ cm}^{-1}$; CDF 2^4 , $A = 24.4 \text{ cm}^{-1}$). Note that the A constant of the 2^6 level of CDF is not as large as CHF 2^4 ($37.5 \text{ vs. } 51.8 \text{ cm}^{-1}$); however, the density of states is higher. Another view is provided in Fig. 4, which compares the fluorescence lifetimes of CHF and CDF averaged over rotational (J) state and plotted on the same energy scale. Obviously, the lifetime lengthening is more pronounced for CHF, and the lifetime data supports the thresholds discussed above.

Fig. 5 displays a plot of A rotational constant vs. quanta of bend for levels in all three progressions, which illustrates the dramatic increase with bending excitation observed also in the case of CHF.^{47,66} Due to extensive RT perturbations in all sub-bands with $K'_a \geq 1$, the A constants could not be determined for levels with $n > 6$.

Vibrational analysis

The vibrational spacings observed for the pure bending levels 2_0^n show the expected linear dependence on n up to approximately $n = 7$, as shown in the upper panel of Fig. 6. As described by Dixon,⁷⁶ the bending vibrational intervals reach a minimum at the barrier, increasing above it, and thus a plot of the vibrational intervals vs. the mean vibronic energy (Dixon plot) exhibits a minimum at the barrier. Such a plot is shown for $n = 6-9$ in the lower panel of Fig. 6, and a minimum is

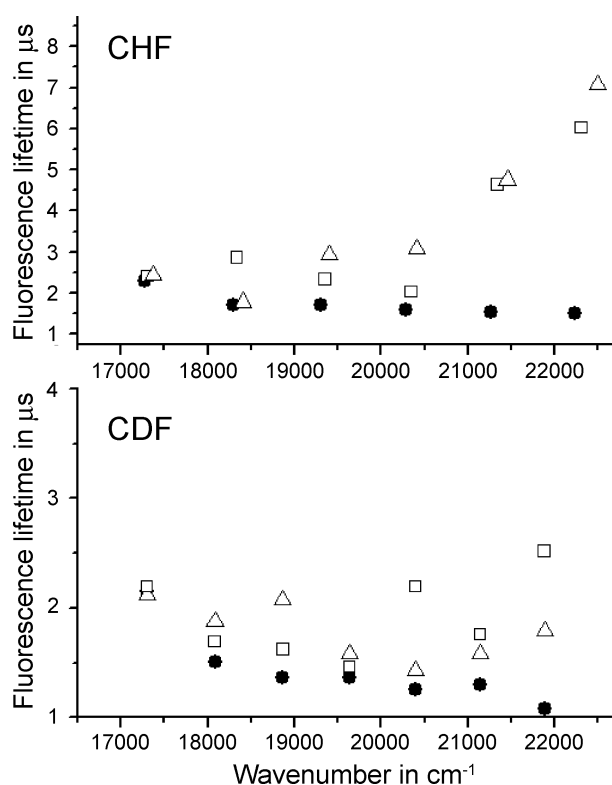


Fig. 4 Average fluorescence lifetimes of the pure bending levels in the \tilde{A}^1A'' state of CHF (upper panel) and CDF, plotted as a function of energy. Legend: ●, $K' = 0$; □, $K' = 1$; △, $K' = 2$.

indeed observed very close to $n = 9$. To estimate the barrier height, we initially followed the procedure used in our previous study of CHF,⁶⁶ fitting the intervals for $n = 6-9$ to a quadratic function using a non-linear least squares routine.

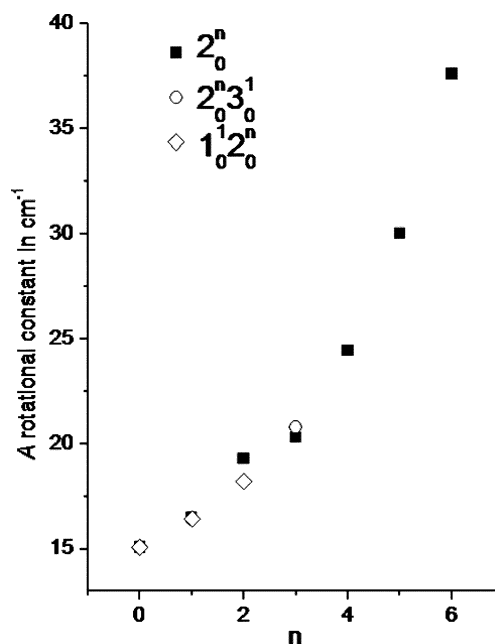


Fig. 5 Dependence of the A rotational constant in CDF(\tilde{A}^1A'') on quanta of bending excitation. The error bars are in each case smaller than the symbol size.

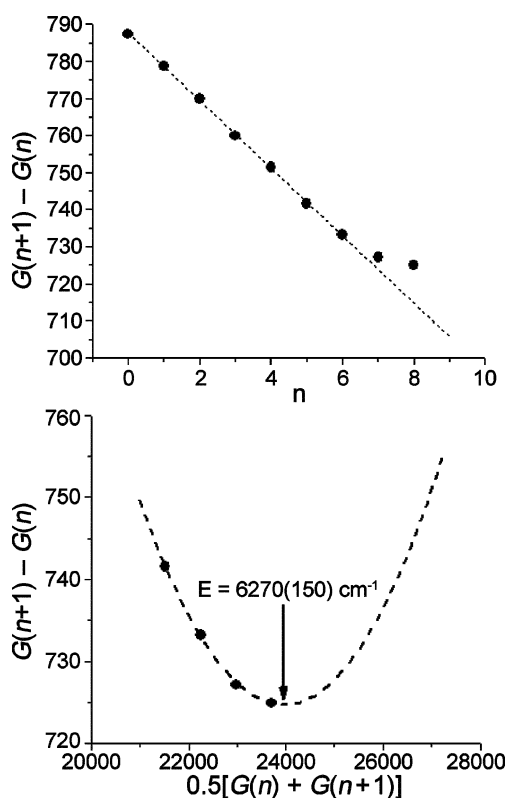


Fig. 6 Upper panel: Plot of the vibrational intervals for the pure bending states 2_0^n vs. quanta of bending excitation. A linear fit of the data up to 2_0^7 is shown. Lower panel: Dixon plot of the vibrational intervals for the pure bending states 2_0^n in the region near the minimum. The line indicates the result of a quadratic fit to the data.

The best fit function is shown as a dashed line in the lower panel of Fig. 6, and the position of the minimum gives a barrier height of $6270 \pm 150 \text{ cm}^{-1}$ above the vibrationless level, compared with a value of $6300 \pm 270 \text{ cm}^{-1}$ determined for CHF and the (zero point corrected) theoretical estimate of 6777 cm^{-1} .⁴⁴

The quadratic function used above was chosen for simplicity, as the data set is limited in the region of the minimum. However, in recent studies of CHBr, where the minimum occurs closer to the center of the Franck–Condon envelope, we find that the full Dixon plots are well fit by a third-order polynomial. We thus fit the complete CHF 2_0^n data set to this function using a non-linear least squares routine, and the result is shown in the lower panel of Fig. 7. The minimum in this function gave a barrier height of $6950 \pm 180 \text{ cm}^{-1}$ above the vibrationless level, larger than that determined above and in better agreement with the theoretical value.⁴⁴

The upper panel of Fig. 7 shows a Dixon plot of the data for the $1_0^1 2_0^n$ progression, together with a fit to a third-order polynomial. Although not as extensive as the 2_0^n set, this data provides the opportunity to test for stretch–bend interactions. The minimum in the fit gives a barrier height of $7900 \pm 90 \text{ cm}^{-1}$ above the vibrationless level, or $5800 \pm 90 \text{ cm}^{-1}$ above the position of the 1^1 level, indicating significant stretch–bend interactions in the excited state.

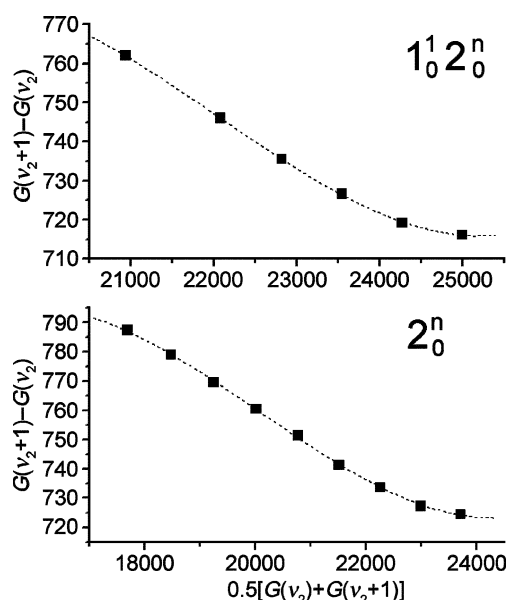


Fig. 7 Lower panel: Dixon plot of the vibrational intervals for the pure bending states 2_0^n (points) together with a third order polynomial fit (dashed line). Upper panel: Similar plot for data from the $1_0^1 2_0^n$ progression.

The vibrational frequencies, excluding those levels near the barrier which deviate from simple anharmonic behavior, were fit using a non-linear least squares routine to a standard anharmonic function (Dunham expansion) of the form⁷⁷

$$G^0(v_1, v_2, v_3) = v_1\nu_1^0 + v_2\nu_2^0 + (v_2)^2x_{22}^0 + v_3\nu_3^0 + v_1v_2x_{12}^0 + v_2v_3x_{23}^0 + v_1v_3x_{13}^0, \quad (1)$$

where ω_i^0 is the harmonic frequency of mode i , ν_i^0 is the anharmonic frequency of mode i , x_{ii}^0 is a diagonal anharmonicity constant, and x_{ij}^0 is a cross-anharmonicity constant. Only levels with single quanta of excitation in v_1 and v_3 were observed; the derived frequencies are anharmonic values. The fit incorporated 18 vibrational levels (including the term energy of 1^1 derived from the 1_1^1 band), and yielded a standard deviation of 2.3 cm^{-1} . The fit parameters are compared in Table 2 with our previous results for CHF.⁶⁶

Hot bands

We did not observe hot bands in our previous study of CHF.⁶⁶ However, for CDF some very weak hot bands were observed, originating from the ground state levels 1_1 , 2_1 , and $1_1 2_1$. Identification of hot bands was aided by the ground state

Table 2 Derived CDF($\tilde{A}^1 A''$) vibrational parameters

Parameter	CDF/ cm^{-1}	CHF/ $\text{cm}^{-1 a}$
ν_1^0	2105.7(17)	2784.9(24)
ω_2^0	792.7(6)	1029.9(8)
ν_3^0	1251.5(18)	1270.8(17)
x_{12}^0	-13.6(4)	-36.6(6)
x_{22}^0	-4.7(1)	-7.5(2)
x_{23}^0	-11.2(6)	-10.0(10)

^a From ref. 66.

Table 3 Fit parameters (in cm^{-1}) for the CDF(\tilde{A}^1A'') hot bands measured in this work

Band	T	A''	$(B'' + C'')/2$	$(B'' - C'')/2$	N^b	σ^c
$1_0^1 2_0^2$	16 897.86(6) ^a	8.67(7)	1.050(8)	0.067(8)	34	0.053
$1_1^1 2_1^1$	17 184.32(6)	8.60(9)	1.044(15)	0.087(15)	18	0.038
1_1^1	17 434.87(8)	14.57(4) ^d	0.971(7) ^d	0.036(7) ^d	29	0.078
2_1^1	17 803.99(8)	9.03(10)	1.052(11)	0.067(11)	24	0.055
$1_1^1 2_0^1$	18 211.48(13)	8.65(16)	1.052(19)	0.084(19)	18	0.082

^a Three standard errors given in parentheses. ^b Number of transitions included in the fit. ^c Standard deviation of the fit. ^d Upper state values; lower state constants were fixed to the values derived for $1_0^1 2_0^2$.

vibrational term energies derived from our DF study.⁷⁰ The bands were analyzed and the resulting fit parameters are listed in Table 3. The term energies combined with data from the cold bands gave the following ground state vibrational term energies (in cm^{-1} , with associated errors derived *via* propagation): 1_1 , 1967.4(12); 2_1 , 1062.1(1); $1_1 2_1$, 2993.7(1). These values are in good agreement with, but more precise than, the values derived from our DF study.⁷⁰

Conclusions

We have recorded and analyzed fluorescence excitation spectra of cold bands involving the pure bending levels 2_0^n with $n = 0-9$ and the combination states $1_0^1 2_0^n$ with $n = 1-8$ and $2_0^1 3_0^1$ with $n = 0-5$ in the $\tilde{A}^1A'' \leftarrow \tilde{X}^1A'$ system of CDF, in addition to some weak hot bands. Fluorescence lifetime measurements were performed for many levels, in order to examine RT induced lifetime lengthening. The derived \tilde{A} state parameters were compared with our previous results for CHF and with the predictions of *ab initio* electronic structure theory. The approach to linearity in the \tilde{A} state is evidenced in a sharp increase in the A rotational constant, and a minimum in the vibrational intervals near 2_0^1 . A fit of the vibrational intervals for the pure bending levels yields a barrier to linearity in good agreement with that derived for CHF and with *ab initio* predictions. As shown in the spectra and lifetime measurements, numerous perturbations were found in subbands with $K'_a \geq 1$, particularly at higher energies, arising from interactions with background levels of both \tilde{X}^1A'' and \tilde{a}^3A'' . From the spectra and lifetime measurements, the onset of strong RT effects is found to occur at a higher energy than in CHF, consistent with the smaller A constant. The analysis of perturbations in this system will be the subject of future work.

Acknowledgements

The National Science Foundation (Grant CHE-0353596) and the donors of the Petroleum Research Fund of the American Chemical Society are gratefully acknowledged for support of this research. The authors thank Dr Rajendra Rathore and Sameh Abdelwahed for assistance in the synthesis of CD_3F .

References

- (a) *Carbenes, in the Reactive Intermediates in Organic Chemistry Series*, ed. R. A. Moss and M. Jones, Jr, Wiley-Interscience, New York, 1973, vol. I; (b) *Carbenes, in the Reactive Intermediates in Organic Chemistry Series*, ed. R. A. Moss and M. Jones, Jr, Wiley-Interscience, New York, 1975, vol. II.

- W. Kirmse, *Carbene Chemistry*, Academic, New York, 2nd edn, 1971.
- J. C. Sciano, in *Handbook of Organic Photochemistry*, CRC Press, Boca Raton, FL, 1989, vol. 2, ch. 9.
- F. A. Carey and R. J. Sundberg, in *Advanced Organic Chemistry, Part 3*, Plenum, New York, 3rd edn, 1990.
- U. E. Weirsum and L. W. Jenneskens, in *Gas Phase Reactions in Organic Synthesis*, ed. Y. Vallée, Gordon and Breach, Australia, 1997.
- A. M. Dean and J. W. Bozzelli, in *Gas-phase Combustion Chemistry*, ed. W. C. Gardiner, Jr, Springer, New York, 2000, ch. 2.
- A. J. Merer and D. N. Travis, *Can. J. Phys.*, 1966, **44**, 1541.
- A. J. Merer and D. N. Travis, *Can. J. Phys.*, 1966, **44**, 525.
- R. Hoffmann, G. D. Zeiss and G. W. Van Dine, *J. Am. Chem. Soc.*, 1968, **90**, 1485.
- M. E. Jacox and D. E. Mulligan, *J. Chem. Phys.*, 1969, **50**, 3252.
- J. F. Harrison, *J. Am. Chem. Soc.*, 1971, **93**, 4112.
- V. Staemmler, *Theor. Chim. Acta*, 1974, **35**, 309.
- C. W. Bauschlicher, Jr, H. F. Schaefer III and P. S. Bagus, *J. Am. Chem. Soc.*, 1977, **99**, 7106.
- N. C. Baird and K. F. Taylor, *J. Am. Chem. Soc.*, 1978, **100**, 1333.
- S. Koda, *Chem. Phys. Lett.*, 1978, **55**, 353.
- R. I. Patel, G. W. Stewart, K. Casleton, J. L. Gole and J. R. Lombardi, *Chem. Phys.*, 1980, **52**, 461.
- C. W. Bauschlicher, Jr, *J. Am. Chem. Soc.*, 1980, **102**, 5492.
- M. Kakimoto, S. Saito and E. Hirota, *J. Mol. Spectrosc.*, 1981, **88**, 300.
- T. Suzuki, S. Saito and E. Hirota, *J. Mol. Spectrosc.*, 1981, **90**, 447.
- P. H. Mueller, N. G. Rondan, K. N. Houk, J. F. Harrison, D. Hooper, B. H. Willen and J. F. Liebman, *J. Am. Chem. Soc.*, 1981, **103**, 5049.
- E. Hirota, *Faraday Discuss. Chem. Soc.*, 1981, **74**, 87.
- M. Kakimoto, S. Saito and E. Hirota, *J. Mol. Spectrosc.*, 1983, **97**, 194.
- R. J. Butcher, S. Saito and E. Hirota, *J. Chem. Phys.*, 1984, **80**, 4000.
- T. Suzuki, S. Saito and E. Hirota, *Can. J. Phys.*, 1984, **62**, 1328.
- K. Hakuta, *J. Mol. Spectrosc.*, 1984, **106**, 56.
- T. Suzuki and E. Hirota, *J. Chem. Phys.*, 1986, **85**, 5541.
- G. E. Scuseria, M. Durán, R. G. A. R. MacLagan and H. F. Schaefer III, *J. Am. Chem. Soc.*, 1986, **108**, 3248.
- E. A. Carter and W. A. Goddard III, *J. Phys. Chem.*, 1987, **91**, 4651.
- E. A. Carter and W. A. Goddard III, *J. Chem. Phys.*, 1988, **88**, 1752.
- K. K. Murray, D. G. Leopold, T. M. Miller and W. C. Lineberger, *J. Chem. Phys.*, 1988, **89**, 5442.
- S. K. Shin, W. A. Goddard III and J. L. Beauchamp, *J. Phys. Chem.*, 1990, **94**, 6963.
- S. K. Shin, W. A. Goddard III and J. L. Beauchamp, *J. Chem. Phys.*, 1990, **93**, 4986.
- B. Weis, P. Rosmus, K. Yamashita and K. Morokuma, *J. Chem. Phys.*, 1990, **92**, 6635.
- G. L. Gutsev and T. Ziegler, *J. Phys. Chem.*, 1991, **95**, 7220.
- M. K. Gilles, K. M. Ervin, J. Ho and W. C. Lineberger, *J. Phys. Chem.*, 1992, **96**, 1130.
- K. K. Irikura, W. A. Goddard, III and J. L. Beauchamp, *J. Am. Chem. Soc.*, 1992, **114**, 48.
- N. Russo, E. Sicilia and M. Toscano, *J. Chem. Phys.*, 1992, **97**, 5031.

- 38 A. Gobbi and G. Frenking, *J. Chem. Soc., Chem. Commun.*, 1993, 1162.
- 39 B.-C. Chang and T. J. Sears, *J. Chem. Phys.*, 1995, **102**, 6347.
- 40 B.-C. Chang and T. J. Sears, *J. Mol. Spectrosc.*, 1995, **173**, 391.
- 41 V. M. Garcia, O. Castell, M. Reguero and R. Collol, *Mol. Phys.*, 1996, **87**, 1395.
- 42 B.-C. Chang and T. J. Sears, *J. Chem. Phys.*, 1996, **105**, 2135.
- 43 B.-C. Chang, R. Fei and T. J. Sears, *J. Mol. Spectrosc.*, 1997, **183**, 341.
- 44 T. W. Schmidt, G. B. Bacskay and S. H. Kable, *Chem. Phys. Lett.*, 1998, **292**, 80.
- 45 A. J. Marr, S. W. North, T. J. Sears, L. Ruslen and R. W. Field, *J. Mol. Spectrosc.*, 1998, **188**, 68.
- 46 D. Das and S. L. Whittenburg, *J. Mol. Struct. (THEOCHEM)*, 1999, **492**, 175.
- 47 T. W. Schmidt, G. B. Bacskay and S. H. Kable, *J. Chem. Phys.*, 1999, **110**, 11277.
- 48 M. Schwartz and P. Marshall, *J. Phys. Chem. A*, 1999, **103**, 7900.
- 49 A. J. Marr and T. J. Sears, *J. Mol. Spectrosc.*, 1999, **195**, 367.
- 50 A. J. Marr and T. J. Sears, *Mol. Phys.*, 1999, **97**, 185.
- 51 B.-C. Chang, M. L. Costen, A. J. Marr, G. Ritchie, G. E. Hall and T. J. Sears, *J. Mol. Spectrosc.*, 2000, **202**, 131.
- 52 H.-G. Yu, T. Lezana-Gonzalez, A. J. Marr, J. T. Muckerman and T. J. Sears, *J. Chem. Phys.*, 2001, **115**, 5433.
- 53 C.-W. Chen, T.-C. Tsai and B.-C. Chang, *Chem. Phys. Lett.*, 2001, **347**, 73.
- 54 T.-C. Tsai, C.-W. Chen and B.-C. Chang, *J. Chem. Phys.*, 2001, **115**, 766.
- 55 C.-W. Chen, T.-C. Tsai and B.-C. Chang, *J. Mol. Spectrosc.*, 2001, **209**, 254.
- 56 H.-G. Yu, J. T. Muckerman and T. J. Sears, *J. Chem. Phys.*, 2002, **116**, 1435.
- 57 C.-L. Lee, M.-L. Liu and B.-C. Chang, *J. Chem. Phys.*, 2002, **117**, 3263.
- 58 A. Lin, K. Kobayashi, H.-G. Yu, G. E. Hall, J. T. Muckerman, T. J. Sears and A. J. Merer, *J. Mol. Spectrosc.*, 2002, **214**, 216.
- 59 B.-C. Chang, J. Guss and T. J. Sears, *J. Mol. Spectrosc.*, 2003, **219**, 136.
- 60 C.-L. Lee, M.-L. Liu and B.-C. Chang, *Phys. Chem. Chem. Phys.*, 2003, **5**, 3859.
- 61 K. Nauta, J. S. Guss, N. L. Owens and S. H. Kable, *J. Chem. Phys.*, 2004, **120**, 3517.
- 62 J. Liang, X. Kong, X. Zhang and H. Li, *J. Mol. Struct. (THEOCHEM)*, 2004, **672**, 133.
- 63 C.-S. Lin, Y.-E. Chen and B.-C. Chang, *J. Chem. Phys.*, 2004, **121**, 4164.
- 64 H. Fan, I. Ionescu, C. Annesley and S. A. Reid, *Chem. Phys. Lett.*, 2003, **378**, 548.
- 65 H. Fan, I. Ionescu, C. Annesley, J. Cummins, M. Bowers and S. A. Reid, *J. Mol. Spectrosc.*, 2004, **108**, 3732.
- 66 H. Fan, I. Ionescu, C. Annesley, J. Cummins, M. Bowers, J. Xin and S. A. Reid, *J. Phys. Chem. A*, 2004, **108**, 3732.
- 67 I. Ionescu, H. Fan, C. Annesley, J. Xin and S. A. Reid, *J. Chem. Phys.*, 2004, **120**, 1164.
- 68 H. Fan, I. Ionescu, J. Xin and S. A. Reid, *J. Chem. Phys.*, 2004, **121**, 8869.
- 69 I. Ionescu, H. Fan, E. Ionescu and S. A. Reid, *J. Chem. Phys.*, 2004, **121**, 8874.
- 70 H. Fan, C. Mukarakate, M. Deselnicu, C. Tao and S. A. Reid, *J. Chem. Phys.*, 2005, **123**, 014314.
- 71 W.-Z. Chang, H.-J. Hsu and B.-C. Chang, *Chem. Phys. Lett.*, 2005, **413**, 25.
- 72 J. S. Guss, C. A. Richmond, K. Nauta and S. H. Kable, *Phys. Chem. Chem. Phys.*, 2005, **7**, 100.
- 73 G. Duxbury, in *Molecular Spectroscopy*, The Chemical Society, London, 1975, vol. 3, ch. 7.
- 74 R. H. Judge and D. J. Clouthier, *Comput. Phys. Commun.*, 2001, **135**, 293.
- 75 W. F. Edgell and L. Parts, *J. Am. Chem. Soc.*, 1955, **77**, 5515.
- 76 R. N. Dixon, *Trans. Faraday Soc.*, 1964, **60**, 1363.
- 77 G. Herzberg, *Molecular Spectra and Molecular Structure III. Electronic Spectra of Polyatomic Molecules*, Van Nostrand, New York, 1966.